Chapter 1. Principles of Synthetic Aperture Radar

Samuel W. (Walt) McCandless, Jr.
SEASAT Program Manager
User Systems Enterprises, Inc., Denver, CO, USA

Christopher R. Jackson
Radar Imaging Resources, Alexandria, VA USA

1.1 Introduction

Beginning with the launch of SEASAT in 1978, synthetic aperture radar (SAR) satellites have provided a wealth of information on such diverse ocean phenomena as surface waves, internal waves, currents, upwelling, shoals, sea ice, wind, and rainfall. The influence of man in the form of offshore facilities, ship transits, and other ocean-related events and artifacts is also observed from space using fine resolution SAR. Although aircraft-based imaging radar had been around since the 1960s, it was unable to provide the wide area global perspective and temporal coverage necessary to observe many ocean processes. Indeed, SAR is the premier sensor for the detection of such phenomena because it is sensitive to small surface roughness changes on the order of the radar wavelength (1 m down to several centimeters). It is also independent of solar illumination and is generally unaffected by cloud cover. In addition, SAR has the advantage of providing control over such factors as power, frequency, phase, polarization, incident angle, spatial resolution and swath width, all of which are important when designing and operating a system for the extraction of quantitative information.

SEASAT, launched in June 1978, was the first civilian SAR satellite. Since then, Canada, Europe, Japan, and Russia (the former Soviet Union) have placed SAR satellites in orbit for investigation and monitoring of both the sea and land surface. The ongoing operation of ERS-2, RADARSAT-1, and ENVISAT, along with currently planned SAR missions, means that SAR data will be available for at least the next decade at X- (3 cm), C- (6 cm), and L-band (24 cm) wavelengths. While each system has its own configuration, in terms of frequency, polarization, resolution, swath width, etc., the underlying operating concept for each is the same.

This chapter presents the principles behind the operation of a SAR. It begins with a historical look at the development of SAR and the evolution of spaceborne SARs. The concepts behind radar operation and aperture synthesis are then presented, along with the factors and limitations that govern SAR performance. A discussion of SAR image formation follows and the chapter concludes with an examination of some basic SAR image characteristics.

1.2 Imaging From Space

Fine resolution remote sensing of earth surface phenomena was first accomplished from space in the 1960s on military and National Aeronautics and Space Administration (NASA) satellites using cameras and camera-like imaging devices (passive radiometers). These early remote sensors in space were used to collect and discriminate radiated and reflected electromagnetic energy in the visible or infrared spectra (roughly 0.4-micron to 20-micron wavelengths). In 1973, the NASA Earth Resource Technology Satellite (ERTS-1), later renamed LANDSAT, initiated a series of missions featuring fine resolution (10s of meters) optical

imagers with many visible and infrared channels that were thematically associated with specific land applications. The LANDSAT satellites continue operation to this day. Although these radiometers are capable of providing fine surface spatial resolution and excellent multi-spectral details, they are inhibited by clouds and depend on solar illumination, and are thus limited to daylight observation. The limitations of clouds and darkness can be overcome by moving to the microwave portion of the spectrum. Microwaves are capable of passing through the clouds and permitting unobstructed observations of the earth's surface, including day or night detection. However, it is virtually impossible for a passive microwave radiometer to achieve the fine resolution produced by devices operating at optical wavelengths.

The diffraction limited angular extent (and subsequent spatial resolution) of an aperture is directly proportional to wavelength and inversely proportional to aperture dimension[1]. From a spacecraft in orbit, a few 10s of meters of resolution at visible and infrared wavelengths can be achieved with a camera aperture of only a few 10s of centimeters. When the wavelength increases from the visible and infrared to microwaves (microns to centimeters), resolution will decrease (become coarser) unless the antenna apertures are increased an equivalent amount. To achieve the same 10s of meters of resolution at microwave frequencies, a spacecraft would need an antenna aperture dimension on the order of 10s of kilometers! In satellite sensor design, this antenna dimension is ridiculously impractical. Both active and passive microwave instruments suffer from this resolution problem; however, for an active microwave instrument (i.e., radar), a technique has been developed to overcome this limitation.

The very limiting factor for a microwave antenna, poor spatial resolution resulting from a large beam width or angular field of view, can be turned to an advantage for a radar that has the ability to precisely measure phase and Doppler. For a radar that has its beam directed orthogonal to its direction of travel, the large beamwidth will cause an object (or location) on the ground to be illuminated and linearly traversed by the radar beam for a extended period of time (tenths of a second to seconds for spacecraft velocities). During this time, the radar collects phase and Doppler measurements that, through signal processing, allow for an aperture to be constructed or synthesized, equivalent to the distance the physical antenna moves while the location remains in the beam. This is the basic concept behind SAR, details of which are discussed in other sections of this chapter and can be found in greater detail in many of the references cited in Section 1.14 [*Curlander and McDonough,* 1991; *McCandless,* 1989; *Raney,* 1998; *Tomiyasu,* 1978; and *Sullivan,* 2000]. The new synthesized aperture, which can be several orders of magnitude larger than the transmit and receive antenna, makes it possible to produce radar imaging with a few meters of resolution.

Figures 1.1a and 1.1b provide a comparison of a SAR and optical/visible image of the same area around Nantucket Island off the coast of Massachusetts. Although the images were not taken simultaneously, they illustrate some of the differences and similarities of these diverse imaging technologies. Clouds, white beaches and some depth information from the water coloration are visible in the passive optical image. The active SAR image shows dark beaches, along with internal waves, manifestations of bottom topography and other fine scale ocean features.

The all weather, day and night, fine resolution capabilities make radar an ideal remote-sensing instrument for many applications in target detection mapping, as well as earth resources

[1]The Fraunhofer diffraction for a rectangular and circular aperture pattern are worked out in Principles of Optics by Max Born and Emil Wolf [1975]. The radiation pattern for a circular aperture is worked out in Microwave Radar: Imaging and Advanced Concepts by Roger Sullivan [2000]

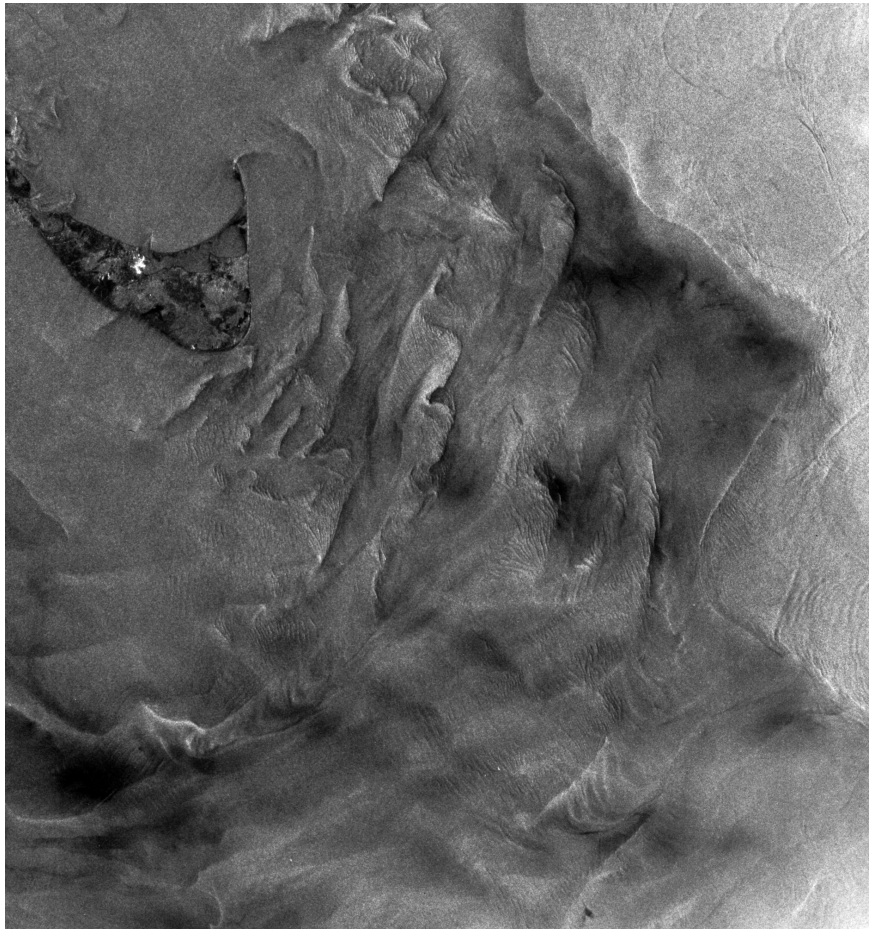

Figure 1.1a. SEASAT (L-band, HH) SAR image of the ocean south and east of Nantucket Island collected on 27 August 1978 (Rev 880, 1234 GMT). The image contains bottom topography, upwelling and internal wave signatures. Image courtesy John Apel [*Evans,* 1995]

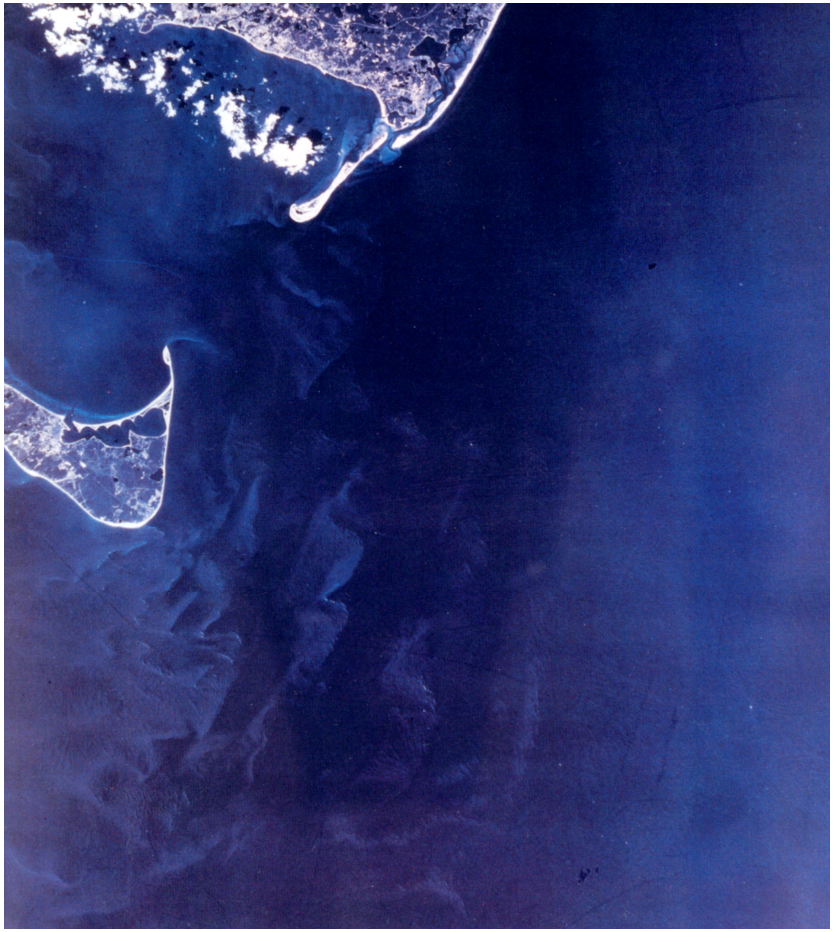

Figure 1.1b. Optical image southeast of Nantucket and Cape Cod collected from Skylab (1973). The image shows the optical signature of shoals and internal waves. Image courtesy John Apel [*Evans,* 1995]

TABLE 1.1: Highlights of SAR History with Space Emphasis

DATE	DEVELOPMENT
1951	Carl Wiley of Goodyear postulates the Doppler beam-sharpening concept.
1952	University of Illinois demonstrates the beam-sharpening concept.
1957	University of Michigan produces the first SAR imagery using an optical correlator.
1964	Analog electronic SAR correlation demonstrated in non-real time (University of Michigan).
1969	Digital electronic SAR correlation demonstrated in non-real time (Hughes, Goodyear, Westinghouse).
1972	Real-time digital SAR demonstrated with motion compensation (for aircraft systems).
1978	First space-borne SAR NASA/JPL SEASAT satellite. Analog downlink; optical and non-real-time digital processing.
1981	Shuttle Imaging Radar series starts - SIR-A. Non-real-time optical processing on ground.
1984	SIR-B. Digital downlink; non-real-time digital processing on ground.
1986	Space-borne SAR Real-time processing demonstration using JPL Advanced Digital SAR processor (ADSP).
1987	Soviet 1870 SAR is placed in earth orbit.
1990	Magellan SAR images Venus.
1990	Evolution of SAR begins in space; Soviet ALMAZ (1991), European ERS-1 (1991), Japanese JERS-1 (1992), SIR-C (1994), ERS-2 (1995), Canadian RADARSAT-1 (1995), SRTM (2000), ENVISAT (2002).

management. Oceanic and ice observations are ideally suited to space-based radar because of the vast geographic scale and the ever-changing nature of the subjects. The ability of radar to penetrate persistent cloud cover over regions important to transport and other commerce have produced improvements in nowcasts, forecasts and climatological analyses because diurnal and seasonal variances can be monitored. Application candidates extend well beyond oceanic and ice observation to include such things as crop and forest monitoring, land management and development, hydrology, disaster management, and an ever-growing list of applications important to science and commerce.

1.3 SAR History

SAR designs and associated applications have grown exponentially since the 1950s when Carl Wiley, of the Goodyear Aircraft Corporation, observed that a one-to-one correspondence exists between the along-track coordinate of a reflecting object (being linearly traversed by a radar beam) and the instantaneous Doppler shift of the signal reflected to the radar by that object. He concluded that a frequency analysis of the reflected signals could enable finer along-track resolution than that permitted by the along-track width of the physical beam itself, which governed the performance of the real aperture radar (RAR) designs of that era.

Satellite	Country	Year	Band	Frequency (GHz)	Wavelength (cm)	Incident Angle (deg)	Polarization	Pulse Bandwidth (MHz) / (Range Resolution (m))	Azimuth Resolution (m) / (Looks)
SEASAT	USA	1978	L-band	1.275	23.5	23	HH	19 / (7.9)	6 / (1)
SIR-A	USA	1981	L-band	1.275	23.5	50	HH	6 / (24.9)	6.5 / (1)
SIR-B	USA	1984	L-band	1.275	23.5	15-65	HH	12 / (12.5)	6 / (1)
ERS-1/2	Europe	1991/95	C-band	5.25	5.7	23	VV	15.5 / (9.7)	25 / (3)
ALMAZ	USSR	1991	S-band	3.0	10	30-60	HH	- / 15*	15 / (2)
JERS-1	Japan	1992	L-band	1.275	23.5	39	HH	15 / (10)	30 / (4)
SIR-C / X-SAR	USA	1994	L-band	1.25	23.5	15 - 55	HH, HV, VH, VV	10 / (15) 20 / (7.5)	7.5 / (1)
			C-band	5.3	5.7				
	Germany		X-band	9.6	3	54	VV		6 / (1)
RADARSAT-1	Canada	1995	C-band	5.3	5.7	20 - 50	HH	11.6 / (12.9) 17.3 / (8.6) 30 / (5)	28 / (4) 50/ (2-4) 100 / (4–8)
SRTM	USA	2000	C-band	5.25	5.7	54	HH, VV	20 / (7.5)	15 / (1)
	Germany		X-band	9.6	3	54	VV	8 / (18.7)	8 – 12 / (1)
ENVISAT	Europe	2002	C-band	5.25	5.7	15 – 45	HH, HV, VH, VV	9 / (16.6)	6 / (1) 150 / (12) 1000 / (18-21)

Table 1.2. Characteristics of Earth orbital SAR systems.

*Based on 0.1 μs uncoded pulse length.

This "Doppler beam-sharpening" concept was exploited by Goodyear and by a group at the University of Illinois. One major problem was implementation of a practical data processor that could accept wide-band signals from a storage device and carry out the necessary Doppler-frequency analysis at each resolvable picture element (pixel). The Illinois group carried out an experimental demonstration of the beam-sharpening concept in 19-52 through use of airborne coherent X-Band pulsed radar, "boxcar" circuitry, a tape recorder, and a frequency analyzer. Table 1.1 provides a brief overview of SAR development and the timeline of orbital missions.

Industrial and military developments, using airborne platforms, continued at Goodyear, Hughes, and Westinghouse. The Jet Propulsion Laboratory (JPL), University of Michigan, Environmental Research Institute of Michigan (ERIM), Sandia Laboratories, and others also began to explore this new technology. In 1974, engineers at JPL formed an alliance with a group of international ocean scientists led by the National Oceanic and Atmospheric Administration (NOAA) to determine if an ocean application satellite featuring a space-based SAR could be achieved. Up until this time, the major emphasis of space-based remote sensing had been on land applications using visible and infrared sensors. The resulting NASA/NOAA alliance assembled a multi-agency, interdisciplinary group of engineers and scientists that focused on ocean and ice applications using active and passive microwave sensors that could collect data day or night with a general disregard for cloud obscuration. From the very beginning, when SEASAT was but a future mission study, this group met regularly as the SEASAT User Working Group chaired by NOAA's Dr. John Apel with JPL's Dr. Alden Loomis serving as his deputy and NASA's coordinator. The SEASAT User Working Group soon expanded to include international participation and continued seamlessly through the program, working diligently to gain the support and funding for such a mission, to define and guide the mission and systems development, and to establish the experiments that would validate the program.

SEASAT [*Lame and Born*, 1982] operated successfully from late June to early October 1978, when it experienced a massive short circuit in the power system. SEASAT was followed by the Shuttle Imaging Radar-A (SIR-A) and Shuttle Imaging Radar-B (SIR-B) flown in 1981 and 1984, respectively [*Elachi et al*., 1986; *Way and Smith*, 1991]. Both the SIR-A and SIR-B radars were variations on the SEASAT radar operating at L-band and HH (horizontal transmit, horizontal receive) polarization. SIR-B had the added capability of operating at different incident angles (the angle of incidence is defined as the angle between the radar line-of-sight and the local vertical at the point where the radar intersects the earth or ocean surface).

With the exception of the Soviet 1870 SAR (not widely distributed), the 1980s saw only Space Shuttle based, SEASAT derivative, spaceborne SAR activity. The 1990s witnessed a significant expansion of SAR missions with the launch of five earth oriented SAR satellites along with two more Shuttle Imaging Radar missions, as well as the pioneering interplanetary use of the Magellan SAR to map Venus. The satellite systems ALMAZ [*Li and Raney*, 1991], European Remote Sensing [ERS-1, *ESA*, 1991], the Japanese Earth Resources Satellite (JERS)-1 [*Nemoto et al*., 1991], ERS-2 [*ESA*, 1995] and RADARSAT-1 [*Raney et al.,* 1991], each operated at a single frequency and single polarization, like SEASAT. ALMAZ and RADARSAT-1 had the added ability to operate at different incident angles. RADARSAT-1 also has a frequently used ScanSAR mode, where the coverage swath extends up to 500 km.

One of the most advanced SAR systems, the Shuttle Imaging Radar-C/X-band SAR (SIR-C/XSAR), was a joint NASA/German Space Agency/Italian Space Agency mission, flown in April and October 1994 on *Endeavor* [*Jordan et al.,* 1991]. The system could be operated

simultaneously at three frequencies (L, C, and X) with the C- and L-band having the ability to alternately transmit and receive at both horizontal and vertical polarization. By collecting a near-simultaneous and mutually coherent version of the scattered field in a minimum basis set of polarizations, this quadrature polarimetry or "fully polarimetric" capability allows for a more complete characterization of the target's scattering characteristics within the illuminated resolution cell area [*Zebker and Van Zyl,* 1991].

The C- and X-band portions of the SIR-C radar were again flown in 2002 for the Shuttle Radar Topography Mission (SRTM). During this flight, a second receiving antenna was placed at the end of a 60-m mast, extended perpendicular to the main radar antenna. The purpose of the mast antenna was to provide a second receiving point in space for each radar pulse. The slight variations in phase, between the receipt of the radar pulses at each of the antennas, will be processed into a height measurement of the reflecting point on Earth's land surface. [*Rosen et al.,* 2000]

Future SAR missions are expected to provide enhanced capabilities, where the radar can be operated in several collection modes. ESA's ENVISAT, the follow-on to ERS-1 and ERS-2, was placed in orbit in March 2002. Like ERS, ENVISAT's ASAR (Advanced SAR) radar operates at C-Band, and has the added capability to collect data in pairs of four polarimetric combinations, as well as operate in a wide-swath (> 400 km) mode. The ENVISAT ASAR has polarimetric diversity, but is not capable of quadrature polarimetry. The upcoming RADARSAT-2 and Japan's ALOS Phased Array L-band SAR (PALSAR) instruments will both have fully polarimetric and ScanSAR operating modes. Table 1.2 provides a list of the earth orbital SAR missions and some of their characteristics. Additional information on these systems and their image products is given in Appendix A of the Manual.

SEASAT began the evolution of space-based SAR that continues to this day. The active international participation of the SEASAT User Working Group led to international cooperation in the form of data collection and processing facilities and experiments with ground truth. In retrospect, the most important result of these cooperative interactions was the zealous expansion of the SAR technology in space. As a result, more than two decades of data collection have provided a rich data source, with each system adding unique characteristics in terms of applications, radar design, and mission data collection parameters.

1.4 Radar And Synthetic Aperture Radar

Radar self-illuminates an area by transmitting pulses of microwave energy. These pulses of radar energy are reflected from the illuminated area and collected by the radar receiver. By precisely measuring the time difference between the transmitted pulse and the receipt of the reflected energy, radar is able to determine the distance of the reflecting object (called range or slant range). The range resolution of a radar system is its ability to distinguish two objects separated by some minimum distance. If the objects are adequately separated, each will be located in a different resolution cell and be distinguishable. If not, the radar return will be a complex combination of the reflected energy from the two objects.

Spatial resolution in the range direction is not range or directly wavelength dependent, but is instead a function of the effective (processed) pulse-width (τ) multiplied by the speed of light (c) and divided by two. Range resolution can also be expressed as the reciprocal of the effective pulse-width (the pulse bandwidth (b)) multiplied by the speed of light

$$\text{Range Resolution} = \left(\frac{ct}{2}\right) = \left(\frac{c}{2b}\right) \quad (1)$$

As the range resolution becomes finer, the pulse bandwidth and data rate grows accordingly. Most modern radars (including SARs) transmit a pulse called a linear frequency modulated (FM) "chirp". The transmitter varies the frequency of the radar pulse linearly over a particular frequency range (an increase in frequency is called an up-chirp). That variation in frequency determines the radio frequency (RF) bandwidth of the system. The chirp length and slope are based on the radar hardware capabilities (RF pulse power, pulse repetition frequency (PRF), Analog-to-Digital (A/D) sampling conversion) and the range resolution requirement. Both real-aperture radar (RAR) and SAR achieve their range spatial resolution in this way. Typical space-borne SAR pulse bandwidths range between 10 and 40 MHz, that produce a slant range resolution, $\frac{c}{2b}$, between 15 and 3.7 meters.

In the direction orthogonal to the radar beam (also called cross range, azimuth, or along track in broadside operation) the SAR is distinctive in its use of aperture synthesis to improve its spatial resolution. By comparison, optical sensors and RARs obtain their resolution through the physical dimensions of their aperture, sometimes referred to as diffraction limited performance. The RAR cross-range spatial resolution is a direct function of radar wavelength (λ) and target range (R) and an inverse function of antenna dimension (D); i.e., proportional to $\left(\frac{l}{D}R\right)$. From space, the RAR range resolution problem can be solved but the poor cross-range or along-track performance, typically kilometers to tens of kilometers, still has to be contended with. One way of achieving better along-track performance is to boost frequency; another is to increase along-track antenna length; a third is to decrease the target range. None of these options are very effective from space. However, by using Carl Wiley's discovery, resolution is determined by the Doppler bandwidth of the received signal, rather than the along-track width of the radar's antenna beam pattern. The along-track resolution of side-looking radar can be of the same order of magnitude as its range resolution. Table 1.3 summarizes the spatial resolution relationship for RAR and SAR systems. The key to converting theoretical groundwork into a "full-bodied" system is an appropriate signal-processing scheme. Fundamental to the SAR concept is the realization that SAR is a marriage of radar and signal processing technologies. This is the key step to understanding the principles upon which SAR is based.

A SAR consists of an end-to-end system that includes conventional radar building blocks such as an antenna, transmitter, receiver, a high technology data collection system providing coherent Doppler phase histories, and a similarly advanced signal processor capable of making an image out of these phase histories. The radar must maintain stringent control of the signal characteristics and collect coherent phase information to allow the construction of the image. **If phase-preserving disciplines are rigidly enforced, a SAR can produce an image whose along-track spatial resolution is largely independent of wavelength and target range.**

In the most basic sense, there must be a translation of either the target through the real radar beam, or the real beam through the target, or a combination of both processes that produce the necessary systematic change of phase in the target's signal during the observation time of the radar. There are many such embodiments of the SAR concept, (phase history variation can also be the result of target rotation, among other causative factors) and new variations of radar/target

TABLE 1.3: Spatial Resolution Functional Relationships

Spatial Direction	SAR	RAR
Cross-Range (Along - Track)	$\frac{\text{Along-Track Antenna Length}}{2}$	$\frac{\text{Wavelength x Target Range}}{\text{Along-Track Antenna Length}}$
Range	$(\frac{c}{2b})$	$(\frac{c}{2b})$

spatial interaction are still being developed. However, the space-based missions outlined in Table 1.2 generally fall under the category in which a single antenna beam is orientated at right angles (broadside) to the radar platform velocity vector so that the side-looking beam scans the target by means of the translating spacecraft platform. This mode of operation is referred to as monostatic strip-mapping. All of the radars listed in Table 1.2 are or were monostatic with the exception of the Shuttle Radar Topography Mission (SRTM). SRTM employed a two-aperture radar with the first antenna transmitting and receiving coupled with a receive-only second antenna located at a precise baseline distance from the first. This arrangement produces interferometric signatures, hence the name IFSAR (or InSAR), capable of being converted into topographic contours and maps.

1.5 SAR Principles

Illustration of a typical space-based, strip-map, monostatic SAR is shown in Figure 1.2 [*McCandless*, 1989]. Consider the string of dots in Figure 1.2 as a set of positions at which the SAR transmits a pulse. Each pulse travels to the target area where the antenna beam intercepts the earth and illuminates targets at that location, and the reflected return pulses are in turn collected by the same antenna. SAR "works" because the radar pulse travels to and from the target at the speed of light, which is much faster than the speed of the spacecraft [*Harger*, 1970]. The SAR system saves the phase histories of the responses at each position as the real beam moves through the scene and then weights, phase shifts, and sums them to focus on one point target (resolution element) at a time and suppress all others. The SAR image signal processing system performs the weighting, shifting, and summing to focus on each point target in turn. It then constructs an image by placing the total energy response obtained in the focusing on a particular target at the position in the image corresponding to that target. SAR achieves a very high signal processing gain because of coherent (in-phase) summation of the range-correlated responses of the radar. All of the signal returns that occur as the real beam moves through each target, as shown in Figure 1.2, can be coherently summed. In many instances, thousands of pulses are summed for each resolution cell resulting in a tremendous increase of the target signal compared to that from a single pulse (a coherent benefit of approximately 4000 for SEASAT SAR). The power from a given scatterer, spread across many pulses (as illuminated) is focused (concentrated) into a single location through processing.

To get some idea of the scale of the data collection and processing challenges faced by spaceborne SAR system designers and operational planners, consider the general magnitude of these subjects for the systems listed in Table 1.2. These SARs transmit more than a thousand pulses per second; illuminate tens of millions of resolution cells (pixels) in the radar beam at

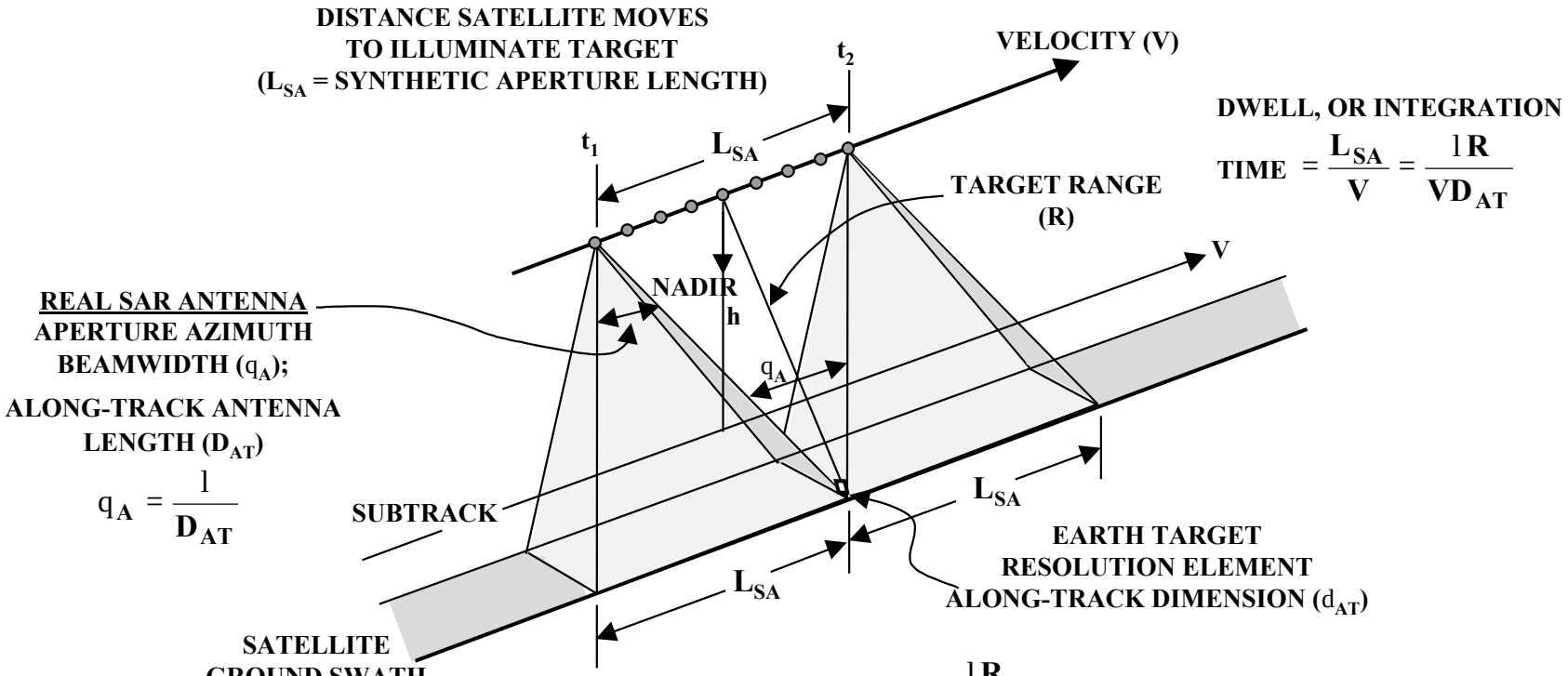

$$L_{SA} = \theta_A R = \frac{\lambda R}{D_{AT}}$$

$$d_{AT} = \frac{\lambda}{2L_{SA}} R = \frac{\lambda R}{\frac{2\lambda R}{D_{AT}}} = \frac{D_{AT}}{2}$$

ACHEIVABLE ALONG-TRACK RESOLUTION IS INDEPENDENT OF RANGE AND RADAR FREQUENCY AND IMPROVES WITH SMALLER REAL ANTENNA APERTURE

Figure 1.2. Basic Principles of Aperture Synthesis

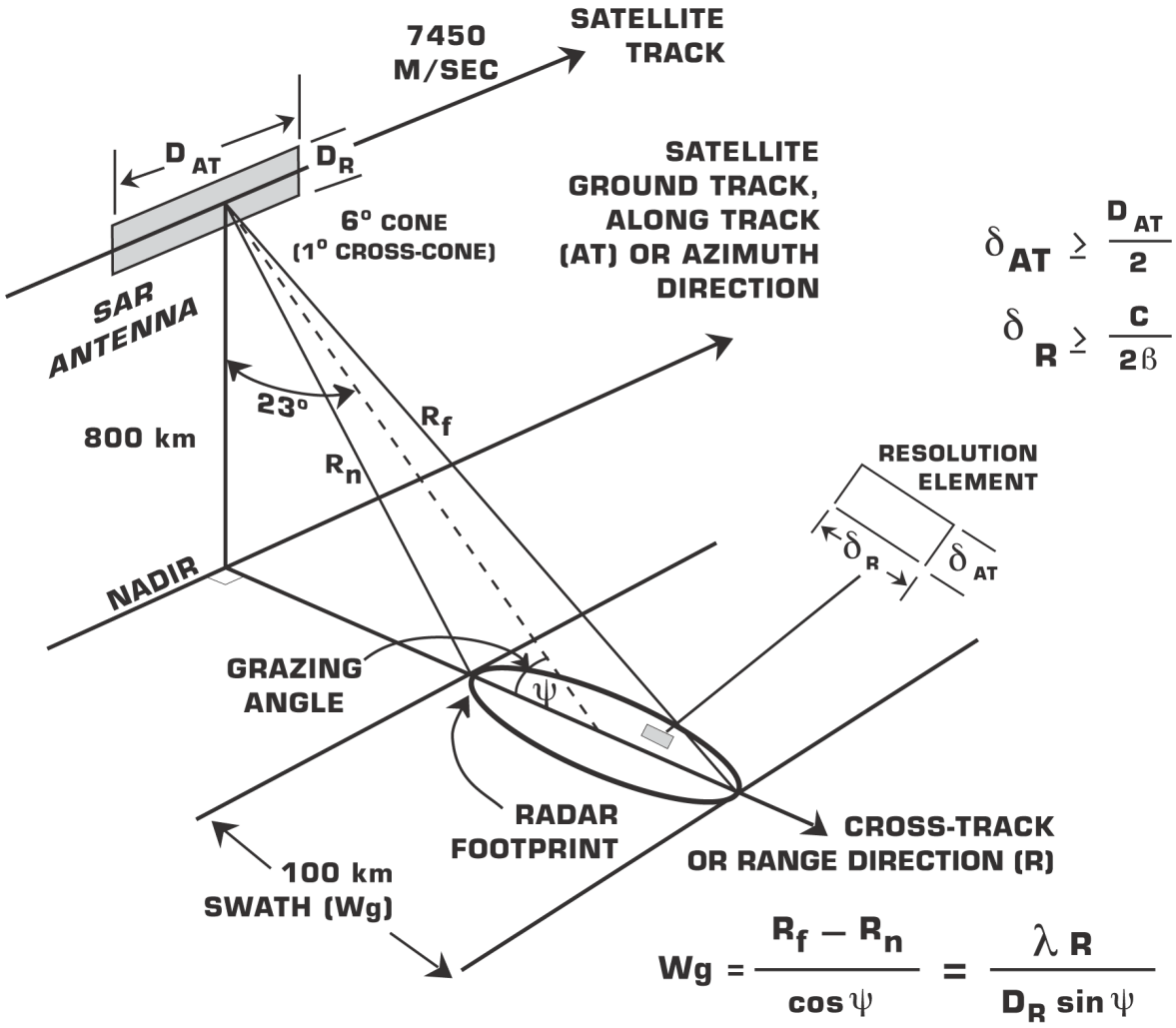

Figure 1.3. SEASAT SAR Imaging Geometry

each pulse time; utilize a spaceborne platform travelling in excess of seven thousand meters per second; and require thousands of processor operations per cell to resolve an image.

When SAR was first introduced on a space platform by SEASAT, optical processing techniques were the touchstone of image generation. Digital processors were limited in numbers and capability and the first digital processors used for SEASAT image generation required 20 hours of processing time to convert an 18-second data collection into a 100-kilometer by 100-kilometer image frame. Although this significant time delay has disappeared as digital technologies and processing skills have advanced, SAR data collection and processing still present great challenges to the satellite and mission designers and are one of the salient yardsticks of program performance and resource allocation.

As indicated, the SAR requires the collection and processing of phase-coherent data and, for an isolated target, the phase history during the integration time follows a complex (higher order) phase function. For descriptive convenience, it is assumed that the radar antenna beam axis is oriented at right angles (broadside) to the radar platform velocity vector. This is the basic orientation of the strip-map SAR systems listed in Table 1.2.

In Figure 1.2, the antenna beam illuminates the target when the platform reaches position t_1, but not before. It continues to illuminate the target for a distance L_{SA} (synthetic aperture length) until it reaches t_2. The time required to translate the along-track beam through a point target is called the integration time or dwell time and is defined in the figure. Figure 1.2 provides a heuristic derivation of the spatial performance result of this process: viz., the spatial resolution in the along-track direction approaches the physical length of the antenna divided by two. This result is, to the first order, independent of the wavelength of the radar and the range from the radar to the target. Unlike the foregoing RAR along-track spatial resolution, the antenna dimension is now a direct, not an inverse, relationship. As a seeming paradox to diffraction limited performance, smaller apertures produce better spatial resolution. All or part of the available phase history can be coherently processed. If all of the pulses are used, the result is referred to as single look, one look, or fully focused processing, achieving a spatial resolution approaching ½ D_{AT}.

Since the along-track resolution is independent of target range, the question is how far can we take this for spaceborne SAR? It will become clear in the next section that there are serious application constraints that limit taking along-track spatial performance too far. These constraints manifest themselves by placing unacceptable limits on important application goals such as area coverage and illumination geometry. There are also associated technology limitations that set application limits. Important technology limitations include data collection rate and volume, and limiting antenna design factors, such as pulse power, phase control and calibration.

Figure 1.3 further illustrates the imaging geometry of a strip-mapping SAR using the illumination geometry of the first space-based SAR, SEASAT. As shown, the length of the synthetic aperture is a function of the beamwidth of the real-aperture, 16 km for SEASAT. In the range direction, the width of the beam as it intercepts the earth is a function of the diffraction-limited beam in the range direction and the illumination geometry. The illumination geometry can be described or specified by either the *look angle* (nadir angle) at the radar, 23 degrees in the case of SEASAT, or by the *grazing angle* where the radar beam intercepts the earth's tangent plane. Sometimes the complement of the look-angle, the *depression angle*, is used for definition or, in the case of the target plane, the complement of the grazing angle (referred to as the *incident angle*) is used as the reference. Using the grazing angle reference, Figure 1.3 provides an expression for swath-width first in terms of diffraction limited beam intersection with the earth and second in terms of the differential range of the target space (the far range minus the near range, $R_f - R_n$). To image the target space illuminated by the radar, each radar pulse will transit the differential range distance twice, first as a transmit-transit and then as a return-transit after target(s) interaction.

1.6 The 2-D Sampling Problem: Ambiguity Relationships

A SAR is a two-dimensional (along-track and range) imaging sensor. This produces a requirement to collect data in the along-track direction and in the range direction that can be processed into an image that is unambiguous (has one solution). Figures 1.2 and 1.3 provide illustrations that help visualize the two-dimensional ambiguity relationships that are so important to SAR applications.

As described, the azimuth resolution of a focused SAR is approximately one half the along-track radar-antenna length, and this resolution is independent of radar frequency and range

(within limits). It would appear that fine along-track resolution could be obtained by simply making the real antenna length very small. This is in fact the case, but ambiguity conditions place certain limits on carrying this too far.

Achieving along-track resolution comes with a requirement that necessitates the radar to send a pulse each time the radar platform translates half of the along-track antenna length. This condition sets the lower bound of the Pulse Repetition Frequency (PRF). The relationship is given by [*Tomiyasu*, 1978]:

$$\frac{2 \times \text{Velocity of Radar}}{Antenna\ Length} < PRF \tag{2}$$

Another way to express this relationship is:

$$\frac{Velocity\ of\ Radar}{\text{Azimuth Resolution}} = \frac{V}{d_{AT}} < PRF \tag{3}$$

Thus, as the along-track antenna length is diminished to improve along-track resolution, the radar must pulse faster. Consequently, there is less time between pulses (the reciprocal of the PRF known as the Inter-Pulse Period or IPP) to collect data in the cross-track or range direction. Unfortunately, only one pulse for a given radar frequency can be in the target zone at a time. Otherwise, range ambiguity occurs, thereby negating two-dimensional imaging. This condition sets an upper bound on the PRF which is a function of the swath width (S = R_f - R_n) in slant range direction as shown in Figure 1.3 and the real (uncompressed) pulse duration, T, resulting in the expression:

$$PRF < \frac{1}{2T + 2(R_f - R_n)/c} \tag{4}$$

More spacing between pulses is required as swath width and/or incident angles increase. Thus, the quest for increased coverage will eventually collide with a desire for improved along-track spatial resolution. For the space-based examples shown in Table 2, the pulse duration, T, is generally much smaller than the swath width time and as a general rule for the single look case [*Raney* 1998]:

$$\frac{V}{d_{AT}} < PRF < \frac{c}{2 \times Swath\ Width} \quad \Rightarrow \quad \frac{2 \times Swath\ Width}{d_{AT}} < \frac{c}{V} \tag{5}$$

In practice there are even more complex considerations of transmit and receive event timing and coordination. For space, several pulses will be in transit simultaneously, and to avoid eclipsing the reflected signals in the monostatic radar, temporal interlacing of returns with the transmitted pulses is required. SAR with interlaced pulses of a particular polarization (i.e., SIR-C, RADARSAT-2), designed to produce polarization specific and unique target signatures, require even more intricate transmit/receive sequences to prevent ambiguous performance.

1.7 Data Rate

All space-based SAR designs have an inherent limitation in the amount of data that can be acquired. Consequently, range resolution, swath width, and dynamic range all vie for resources within this performance limit. Important design elements, such as the satellite to ground link (downlink), analog to digital (A/D) converters, and onboard recorders are still daunted by the voracious resource needs of contemporary spaceborne SAR. SEASAT posed a dilemma in 1978 with its 120 Mega-bit per second (Mbps) data rate when available systems of that era topped out at 15 Mbps. The solution was an innovative analog downlink coupled with a similarly unique ground system capable of converting the data to a digital form and recording it on a SEASAT peculiar 42-channel tape recorder. This end-to-end system was a one-of-a-kind solution never to be used again. Although considerable effort is underway to improve the limiting technologies and SAR designers are searching for ways to more efficiently use available A/D conversion, on-board recording and downlink capabilities, contemporary satellite systems continue to press the limit with 500 Mbps aspirations. Data collection and subsequent processing will continue as one of the most important determinants of systems feasibility and cost; influencing data collection, image signal processing, and ultimately the entire applications process.

The data rate for a full resolution, single look SAR data collection can be described by:

$$\text{Data Rate} = 2\, b_s \mathrm{N} \frac{\text{Swath Width Time}}{\textit{Inter} - \textit{Pulse Period}} \tag{6}$$

Four important performance factors are involved in determining the data rate. They are:

1. The range resolution. The pulse bandwidth (b) of the radar determines its range resolution ($\delta_R = \frac{c}{2b}$). As the pulse bandwidth is increased, and the range resolution becomes smaller, the data sampling (A/D conversion) rate ($2\, b_S$) grows. The data collection or system bandwidth (b_S) will preserve the pulse bandwidth ($b_S > b$).
2. The number of bits per sample (N) sometimes called the quantization rate. The dynamic range (number of useful signal levels) requirement determines how many bits are needed to preserve image data quality.
3. Minimum Inter-Pulse Period. The swath width requirement dictates a minimum length of time, $2(R_f - R_n)/c$, for the Inter-Pulse Period to sustain unambiguous, in range, data collection.
4. Maximum Inter-Pulse Period. The azimuth (along-track) resolution requirement determines the maximum length of the Inter-Pulse Period for unambiguous, in Doppler, data collection.

The SAR designer must select a PRF, or conversely the IPP, consistent with unambiguous operation in range and azimuth. Factors three and four often provide some needed relief in many SAR designs because the time required to collect information from the swath (3) is less than the interpulse period (4) required for azimuth resolution. Positive use of this time advantage reduces data rate and is referred to as time expansion buffering or stretch processing. This technique allowed the SEASAT data rate to be reduced. The SEASAT pulse bandwidth was 19 MHz and the approximate sampling rate of the ground based A/D converter ($2\, b_S$) was 44 mega-samples

per second which, at 5 bits per sample (N), resulted in a 220 Mbps data rate. Factors 3 and 4 allowed this rate to be reduced to 120 Mbps.

As in the case of range and Doppler ambiguities, the applications conflict between swath width and along-track resolution reoccurs in the data rate relationship. As along-track resolution becomes smaller and the swath width grows, the swath width time and interpulse time approaches 1 and time expansion buffering is no longer available to reduce data rates.

Another technique that is very effective and frequently used to reduce the data rate on many space-based SAR (i.e., SIR-C, RADARSAT-2 and most notably the Venus mapping SAR that formed the core of the MAGELLAN mission) is a technique referred to as Block Floating-Point Quantization (BFPQ) [*Johnson*, 1991] or Block Adaptive Quantization (BAQ). The concept of BFPQ is somewhat similar to an Automatic Gain Control (AGC). BFPQ scans a block of phase history data and estimates an overall scale (called the exponent) for the block of data. The block of data is then requantized relative to this scale value (these values are called the mantissas). The block of phase history data is replaced by the quantized exponent and mantissas. For example, the A/D converters on SIR-C produce 8-bits per sample. Blocks of 128, 8-bit samples are compressed into a single 8-bit exponent and 128, 4-bit mantissas, which is nearly a 2:1 compression. The processed imagery products are virtually indistinguishable from products produced from the full 8-bit samples.

SAR systems can use additional techniques to reduce the data rate. One such technique is based on utilizing N_A and N_R, the number of looks in azimuth and range respectively. These refer to the percentage (1/N) of the available azimuth or range bandwidth, respectively, that is used to produce the SAR image. If this is done prior to recording the signal history it is often referred to as presumming. However, most of the systems identified in Table 2 do not use this technique to reduce the recorded signal history or raw data rate because of the attendant loss of spatial resolution that accompanies the reduction of range and/or azimuth bandwidth.

1.8 The SAR Antenna

Antenna technology also paces modern SAR radar design and ambiguity considerations also influence the sizing of the SAR antenna. There exists a minimum antenna area that will assure simultaneous compliance with range and azimuth ambiguity constraints [*Tomiyasu*, 1978].

$$A_{min} = \frac{4 \, \mathrm{V} \, l \, R \tan f_l}{c} \tag{7}$$

The antenna area, as shown in Figure 1.3, is the product of antenna dimensions D_{AT} x D_R . The demand for improved along-track spatial resolution is in contention with achieving wide swath width because it causes the range dimension of the antenna to increase in order to comply with a required minimum antenna dimension for SAR. Conservative SAR designs pay heed to this limit and most of the SAR missions tabulated in Table 2 achieved SAR antenna dimensions of about twice the minimum required by ambiguity constraints.

In addition to the minimum antenna area constraint, there is another ambiguity constraint that is crucially important to space-based SAR. The area cover rate (ACR, area mapped per unit time which equals the product of swath width and platform velocity) is bounded by:

$$ACR < \frac{c}{2} \, Azimuth \; Resolution \tag{8}$$

Thus, the finer the azimuth resolution, the less is the ACR. As we know from the along-track ambiguity and minimum antenna area constraints, finer azimuth resolution implies a larger PRF, which in turn implies a narrower swath. As an example, the ultrafine mode of RADARSAT-2 will have 3 m resolution. The above equation says the swath must not exceed 60 km at an orbital velocity of 7.5 $km \cdot s^{-1}$. Indeed, the designed swath-width is about 45 km, due to data rate constraints. To circumvent this constraint, the SAR must be capable of operating two or more SAR antenna beams simultaneously.

Two basic antenna technologies are currently in use in the SAR systems tabulated in Table 1.2.

1. A constrained (corporate) feed array (planar or modified planar). This system can be pointed electronically although some mechanical redirection may be also incorporated. Example - SEASAT, Space Shuttle SAR (SIR-A and SIR-B), ERS-1, ERS-2, JERS-1, ALMAZ and RADARSAT-1.
2. A distributed array using transmit/receive modules (T/R) that is similar in electrical performance to the corporate feed array. This system has the advantages of better phase control and beam steering. These systems were first introduced by the Space Shuttle SIR-C and SRTM designs and are the basis for the ENVISAT and RADARSAT-2 designs.

The first design uses a centralized RF transmitter and receiver, usually not co-located with the antenna, connected to the antenna via waveguides or coaxial cables. The second design moves the transmit/receive function to the antenna and distributes hundreds to thousands of transmit/receive modules in a nearly uniform pattern as part of the antenna structure to achieve the same result.

1.9 SAR Signal Processing and Image Formation

In a SAR signal processor there are specific operations required to convert a raw data set into an interpretable image. The raw SAR data is not an image since point targets are spread out in range (because of the long frequency coded pulse) and in the along-track dimension (by the real beam moving through the point target for the duration of the dwell time), as shown in Figure 1.2. Figure 1.4 illustrates the raw data trace of a typical point-target as the beam moves in the along-track or azimuth direction. As the radar moves by the target, the radar-to-target range varies, forming the curved trace shown. This translation also produces an along-track frequency/time trace in azimuth, induced by Doppler, and range pulse encoding produces a somewhat similar time/frequency trace in range.

The SAR signal processor compresses this distributed target information in two dimensions (range and along-track) to create the image. The complexity of this process is revealed in Figure 1.5. Figure 1.5a is an example of the raw image data recorded by a SAR system. All of the point targets (δ_R by δ_{AT} resolution elements) that exist in the beam at each pulse instance are superimposed and create a complex interference pattern that is not interpretable in terms of targets and target location. This is the situation that a SAR processor must unravel to produce an image of the sampled scene. Also embedded in the raw data are unwanted distortions and perturbations between the collection platform and the earth that must be accounted for. Examples of distortions and perturbations include range curvature, earth rotation during the integration period, orbit eccentricity, spacecraft attitude noise, among others. As a result, many complex operations must be performed prior to image formation such as platform motion compensation for roll, pitch and yaw offsets, and target motion during the

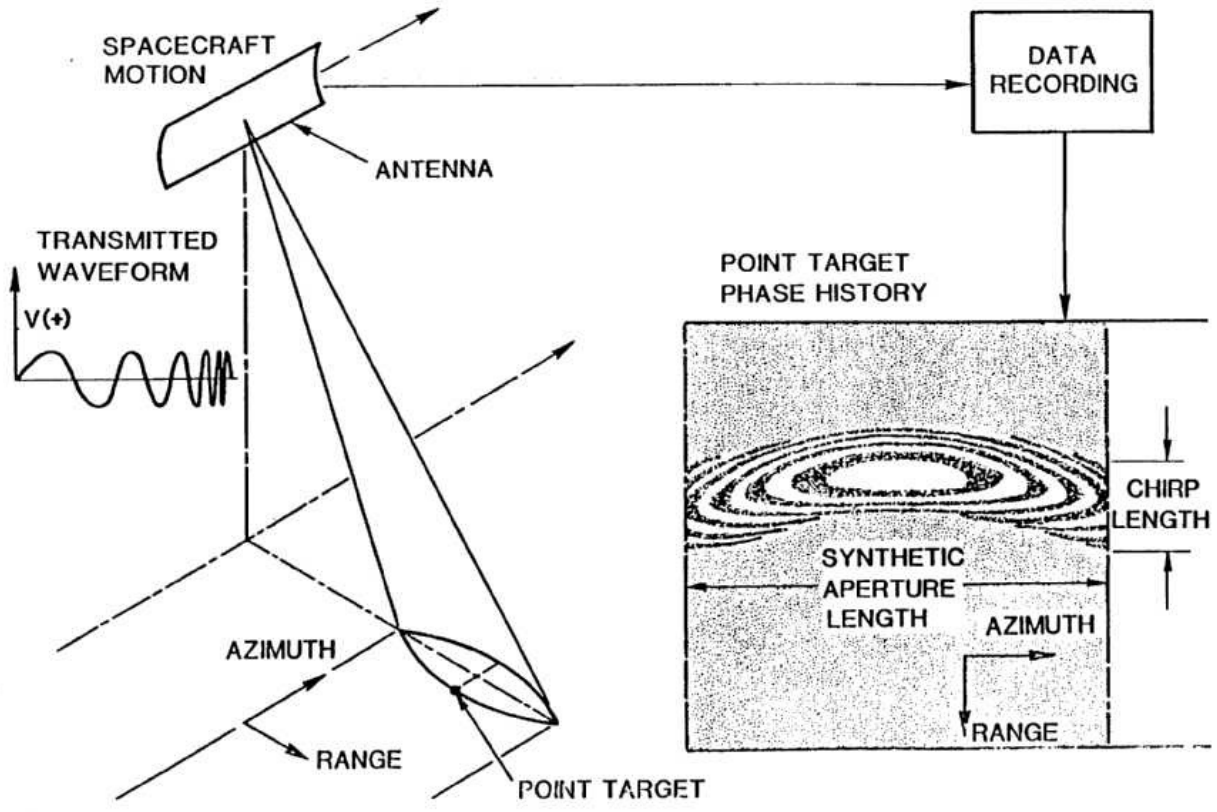

Figure 1.4. SAR Point Target Return

radar/target dwell times. At present, these perturbations or distortions are removed via a series of iterative operations that include attitude/orbit compensations, explicit range-curvature correction algorithms and the option of a variety of applicable auto-focusing techniques. Many advanced space-based SAR designs (e.g., ERS-1 and ERS-2, ALMAZ, RADARSAT-2) normalize the effects of earth rate by using a few degrees (±3 degrees over the course of a typical 90-minute orbit) of programmed yaw steering coordinated with the satellite platform's orbital location. The objective is to steer the real antenna beam to maintain orthogonality to the satellites ground track rather than to the orbit plane. Figure 1.5b and 1.5c show the intermediate step after compressing the distributed target first in range and then the resulting image after compression in azimuth (along-track). Embedded in this process are all of the complex compensations discussed.

Several computation techniques may be used to form a SAR image [*Curlander and McDonough*, 1991]. One method is to use Fourier spectrum estimation techniques, commonly implemented via a "Fast Fourier Transform". Time domain matched filters may also be used. The choice is applications dependent and usually made based on computational efficiencies. In either case, the result is the same; the along-track resolution of the radar is vastly improved compared to real aperture radar and is not dependent, to the first order, on target range or radar wavelength.

In summary, SAR image formation (not to be confused with post image enhancement processing and feature identification) requires many rote processes and computation intensive signal processing of coherent radar return phase histories. To provide a scale of the processing

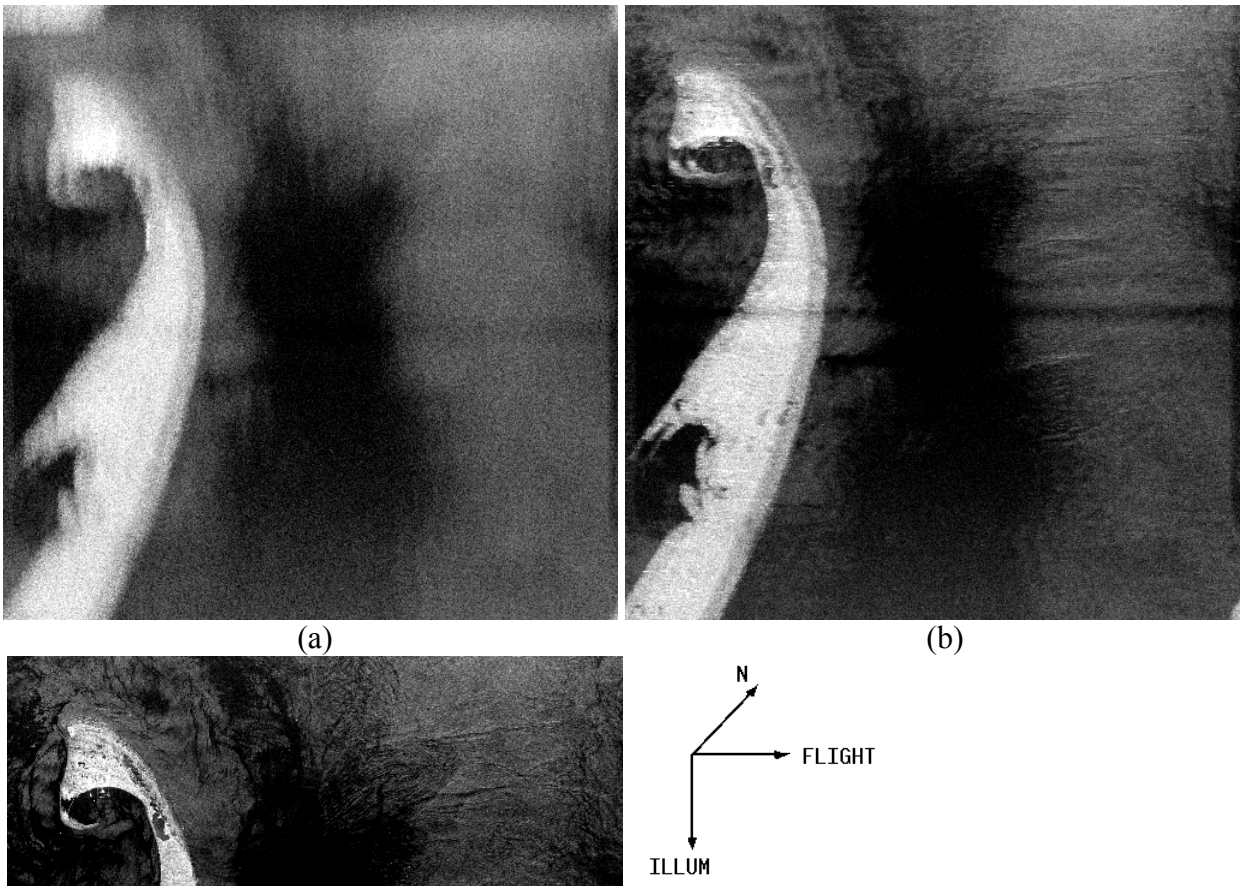

Figure 1.5. SIR-C (L-band, HH) images of the tip of Cape Cod, showing the steps in SAR image formation. (a) is the amplitude of the phase history radar return. The radar energy is spread out over the SIR-C chirp length in range (~10 microsecond or ~3 km) and the synthetic aperture length in azimuth (~1.6 km), so the impulse response from any point target covers roughly 4.8 km^2. (b) is the amplitude image after range compression. (c) is the fully processed image (after azimuth compression). Each imaged area is approximately 38 km (range) x 43 km (azimuth) and centered near 41.9^o N and 70.0^o W. Data were acquired 15 April 1994 (DT 97.2).

burden, consider a single-channel space-based SAR collecting a 100-km swath width image with a space platform collection speed of 7600 meters per second. These values are indicative of many of the systems listed in Table 1.2. Suppose that the SAR is capable of producing a 10-m ground range and 10-m along-track pixel after image processing. The SAR collects over seven million pixels per second and the processor requires more than one thousand operations per pixel to produce the image. A real time or even near real time image processor must be capable of 10^9 complex operations per second or greater as a function of radar and platform complexities. This situation doesn't get less daunting as modern space-based SAR designs reach for enhanced performance. Adding more channels to a radar, in the case of a fully polarized SAR such as RADARSAT-2 (factor of four), or more wavelengths and polarization channels in the case of the space shuttle SIR-C radar (factor of nine) adds to the toll.

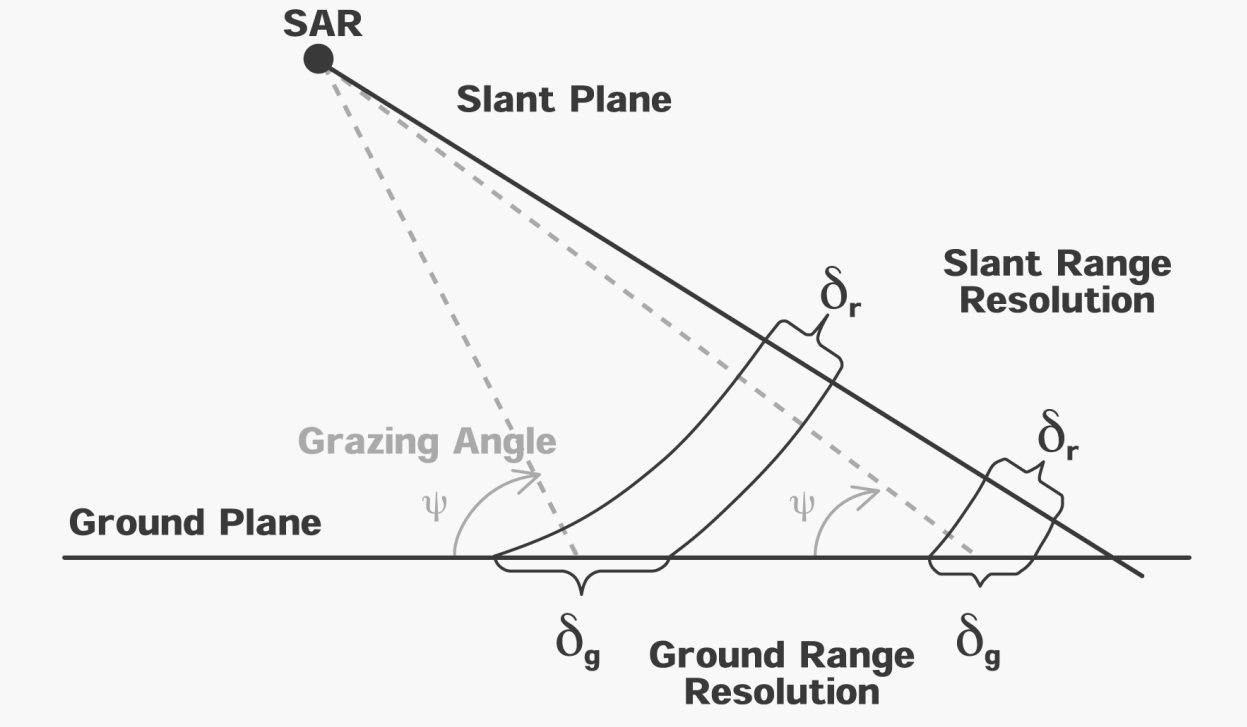

Figure 1.6. Slant plane and ground plane imaging geometry (flat earth).

Although SAR processing is, and will remain, computationally intensive, it offers the advantage of fine cross-range (along-track) spatial resolution with a small antenna, which makes SAR attractive for use on aircraft and satellites. The economic benefits of fine resolution weather independent imagery are significant. The large area of coverage that is possible from space-based radar makes it attractive for many applications, especially for ocean and ice observations for reasons of scale, synoptic variability, impact of weather and climate, and a host of known and emerging reasons with scientific and commercial bearing.

1.10 SAR Image Characteristics: Geometry and Speckle

1.10.1 Slant Plane / Ground Plane

A SAR image has several characteristics that make it unique. The position and proportions of objects in the image can appear distorted compared to a photograph and the image also has a grainy appearance, due to the presence of many black and white pixels randomly distributed throughout the image. Both characteristics result from SARs method of observation (i.e., transmission of a coherent pulse of energy and measurement of its coherent reflection).

A SAR, like any other radar, very precisely measures the time between a transmitted pulse and receipt of its reflection. The pulse travels along a straight line between the radar and surface of the earth. The delay time associated with a particular reflection is converted to distance, and the distance measured along this line of sight is called slant range. A SAR samples its signal in the slant range direction at constant intervals (its resolution in this plane is also constant $\{\frac{c}{2b}\}$). This constant sampling in range, however, does not correspond to a constant sample spacing on the ground (or ground plane). It is this difference in sample spacing between

the slant plane and locations along the ground that produces the unique geometric characteristics of a radar image.

Figure 1.6 shows the SAR viewing geometry and the difference between the slant plane and ground samples. The sample spacing (and resolution) along the ground is a function of the SAR's grazing angle where the grazing angle is defined as the angle between the radar line of sight and the local tangent plane at the point of the reflection on the earth. The resolution in the ground plane image is coarser then the corresponding slant plane image and the relationship between the two is given by:

$$\delta g \sim \delta r / \cos \psi \tag{9}$$

where ψ is the grazing angle. To make a SAR image appear "map-like", the sampling along the slant plane must be converted to the ground plane. Simply converting the slant plane samples to the ground plane will produce ground range pixels of varying size from one end of the swath to the other. Additional resampling is required to produce pixels of equal size.

Slant to ground range distortions are often small for the space-based SARs listed in Table 1.2 because of the small variation in incident angle from the near side to the far side of the swath. For SEASAT, the 6^o variation in angle resulted in an approximate 25% variation in pixel size across the image [*Fu and Holt,* 1982]. These distortions will increase as the angle variation increases across the swath.

1.10.2 Speckle

The grainy "salt and pepper" appearance of a SAR image results from constructive and destructive interference of the coherent SAR pulse by different scatterers contained within a resolution cell. The coherent interaction of electromagnetic radiation with a complicated set of scatterers is probably the least understood and limiting facet of SAR processing system design and application. Noncoherent sensors generally employ diffraction limited physical apertures for the focusing of incident electromagnetic radiation, followed by detectors which are sensitive to the total intensity of the radiation incident upon them. In contrast, a SAR transmits a very precise signal toward its target and, when the reflected radiation returns, a SAR records not only the amplitude of that signal but its phase as well. It is the phase information which allows for the post-facto coherent summation of the many thousands of recorded signals in the correlator during the aperture synthesis operation. Coherent signals have properties that are considerably different from their noncoherent counterparts. The coherent interference between targets contained within a resolution cell is the basis for much of the scintillation of coherent radar imagery—an effect often referred to as speckle. Thus, there is a wide variation in the SAR image, even when given a uniform input. This variation can be considered as a form of noise. However, speckle is not really noise in the classic sense and there is information to be obtained from it because speckle is the radar signature of the target under a particular set of circumstances. A considerable amount of work has gone into speckle characterization and abatement, details of which can be found in *Goodman* [1976], *Lee* [1986], *Lopes et al.,* [1990, 1993], *Arsenault and April* [1986].

1.11 Multi-Look Processing

Multi-look processing involves creating several independent images of an area by sub-dividing or partitioning the available bandwidth spectrum (in either range, azimuth, or both) and then combining those images to produce the final image. The mean Doppler frequency of each

partitioned look is proportional to the time at which the data for that look were collected relative to the local reference time of the Doppler centroid. This is an important concept because it lies at the heart of cross-spectral techniques for suppressing the 180-degree ambiguity in ocean wave directional spectra and in developing techniques for mapping sea surface topography. By partitioning the bandwidth spectrum into N non-overlapping segments, statistically independent images of the scene can be produced and then combined, reducing image speckle. Dividing the bandwidth has the effect of breaking up the coherent nature of the SAR signal. Scatterers that might combine constructively in one part of the bandwidth spectrum may not in another. The price for reducing the coherent scintillation in the image is an attendant decrease in spatial resolution. The benefit lies in the correct interpretation of many dynamic scenes.

A SAR image can be formed using all or part of the signal bandwidth. If the full bandwidth is used, the result, referred to as single look, one look, or fully focused processing, achieves a spatial resolution of ($\frac{c}{2b}$) in range and approaches ½ D_{AT} in the along-track dimension. The multi-look technique can be applied as three-look, four-look, and so on. Speckle is reduced with an increasing number of looks. As a rule of thumb, the standard deviation of the speckle is reduced in proportion to the square root of the number of effective statistically independent looks.

1.12 SAR Imaging and the Ocean Surface

A SAR relies on the precise measurement of phase and Doppler which, through signal processing, allows for its aperture to be synthesized and fine resolution imaging achieved in the along-track direction. The discussion of SAR signal processing and image formation (Section 1.8) contained the assumption that the instantaneous Doppler shift of the signal was the result of transverse movement of the radar beam across the reflecting object. An object's inherent motion (with a component along the radar line of sight) at the time of observation will also produce a Doppler shift and affect how it appears in the resulting SAR image.

The interaction between the SAR pulse of microwave energy and the ocean surface is complex, dependent on wavelength, polarization, geometry, environmental conditions and the electrical properties of the ocean surface. (Details can be found in Chapter 2 and Chapter 4 of this manual). SAR energy is primarily scattered from the ocean surface by the presence of small (mm- to cm-scale) wind-induced surface waves called Bragg waves. SAR is particularly sensitive to the Bragg waves in which wavelength is matched to the projection of the SAR electromagnetic wavelength onto the local ocean surface. A Bragg wave on the ocean surface will cause all of the electromagnetic wavefronts scattered from its different portions to be in phase (i.e., they travel an integral number of wavelengths) and add constructively.

The sea surface is constantly moving and the mean wave structure will include a variety of motions with components along the line-of-sight to the radar. These motions will induce (small) Doppler frequency shifts on the reflected signals. These shifts, and the resulting misregistration of scene scatterers, produce a smearing, or blurring in the azimuth direction. This smearing is like a low pass filter, removing certain ocean wave components. These shifts tend to be different for different phases of the dominant (long) waves and the onset and magnitude of the effect depends primarily on significant wave height, and other parameters. The term given this phenomenon is velocity bunching. It is a fundamentally limiting factor in a SAR's ability to image ocean wave fields (see Chapter 2, Section 2.2.3).

The same effect can be observed from larger objects moving in the scene. For example, ships are observed displaced from the apex of their wake signatures (see Chapter 12, Figure 12.9) or trains appear moved from the location of the tracks.

While motion along the radar line-of-sight limits the imaging ability of a monostatic strip-mapping SAR, a technique called Along Track Interferometry (ATI) takes advantage of these small Doppler shifts to measure line-of-sight velocities (details of ATI can be found in Section 2.4.2). In an ATI SAR system, two antennas are configured such that one is located fore and the second aft in the platform velocity direction. The motion of scatterers can be determined by measuring the phase difference between the signals received at two antennas. The technique has limitations but aircraft-based ATI measurements have been used to examine surface currents and waves.

1.13 Future Trends

In the 25 years since SEASAT, SAR observations of the world's oceans have progressed from a demonstration of capability to near real-time support for operational ice analyses and charting. ERS 1, ERS-2, and RADARSAT-1 have compiled vast archives covering all of the world's oceans, providing observations of surface waves, internal waves, currents, eddies, upwelling, shoals, sea ice, rainfall, the atmospheric boundary layer phenomena, and ships. The evolution sparked by SEASAT continues with ever more advanced SAR satellites beginning with the recent launch of ENVISAT (Europe), followed by ALOS (Japan) and RADARSAT-2 (Canada) in the 2004/2005 time period. These entries promise finer resolution and increased polarimetric capability coupled with advanced data collection and processing techniques (e.g., interferometry) and they will expand SAR capabilities both for the traditional SAR users and for an expanding community of users

1.14 References

Arsenault, H. H., and G. V. April, 1986: Information content of images degraded by speckle. *Opt. Eng.*, **25**, 662–666.

Born, M., and E. Wolf, 1975: *Principles of Optics.* 5th ed. Pergamon, 808 pp.

Curlander, J. C., and R.N. McDonough, 1991: *Synthetic Aperture Radar: Systems and Signal Processing*. John Wiley and Sons, 647 pp.

Elachi, C., J. Cimino, and M. Settle, 1986: Overview of the Shuttle Imaging Radar-B preliminary scientific results. *Science,* **232**, 1511–1516.

ESA, 1991: ERS-1 special issue. *ESA Bulletin*, **65**. [Available from the ESA Publications Division, 8-10 rue-Mario-Nikis, 75738 Paris Cedex 15.]

ESA, 2001: ENVISAT special issue. *ESA Bulletin,* **106**, 168 pp. [Available from the ESA Publications Division, 8-10 rue-Mario-Nikis, 75738 Paris Cedex 15.]

Evans, D. L., Ed., 1995: Spaceborne Synthetic Aperture Radar: Current status and future directions. NASA Tech. Memo. 4679, 171 pp.

Fu, L.-L., and B. Holt, 1982: Seasat views oceans and sea ice with synthetic-aperture radar. Jet Propulsion Laboratory JPL Publ. 81-120, Pasadena, CA, 200 pp.

Goodman, J.W., 1976: Some fundamental properties of speckle. *J. Opt. Soc. Amer.*, **66**, 12 1145–12 1150

Harger, R. O., 1970: *Synthetic Aperture Radar Systems: Theory and Design*. Academic Press, 240 pp.

Johnson, W. T. K., 1991: Magellan imaging radar mission to Venus. *Proc. IEEE*, **79**, 777–790.

Jordan, R. L., B. L. Huneycutt, and M. Werner, 1991: The SIR-C/X-SAR Synthetic Aperture Radar System. *Proc. IEEE,* **79**, 827–838.

Lame, D. B., and G. H. Born, 1982: SEASAT measurement system evaluation: Achievement and limitations. *J. Geophys Res.*, **87** (C5), 3175–3178.

Lee, J. S., 1986: Speckle suppression and analysis for synthetic aperture radar images. *Opt. Eng.*, **25**, 636–643.

Li, F. L., and R. K. Raney, 1991: Prolog to special section on spaceborne radars for earth and planetary observations. *Proc. IEEE,* **79**, 773–776.

Lopes, A., R. Touzi, and E. Nezry, 1990: Adaptive filters and scene heterogeneity. *IEEE Trans. Geosci. Remote Sens*., **28**, 992–1000.

——, E. Nezry, R. Touzi, and H. Laur, 1993: Structure detection and statistical adaptive filtering in SAR images. *Int. J. Remote Sens*., **14**, 1735–1758.

McCandless, S. W., 1989: SAR in Space—The theory, design, engineering and application of a space-based SAR system. *Space Based Radar Handbook,* L. Cantafio, Ed., Artech House, 121–166.

Nemoto, Y., H. Nishino, M. Ono, H. Mizutamari, K. Nishikawa, and K. Tanaka, 1991: Japanese Earth Resources Satellite-1 Synthetic Aperture Radar. *Proc. IEEE,* **79**, 800–809.

Raney, R. K., 1998: Radar Fundamentals: Technical Perspective. *Principles and Applications of Imaging Radar, Manual of Remote Sensing*, F. Henderson and A. Lewis, Eds., 3d. ed., Vol. 2, John Wiley and Sons, 9–130.

——, A. P. Luscombe, E. J. Langham, and S. Ahmed, 1991: RADARSAT. *Proc. IEEE,* **79**, 839–849.

Rosen, P. A., S. Hensley, I. R. Joughin, F. K. Li, S.N. Madsen, E. Rodriguez, and R. M. Goldstein, 2000: Synthetic aperture radar interferometry. *Proc. IEEE*, **88**, 333–382.

Sullivan, R. J., 2000: *Microwave Radar: Imaging and Advanced Concepts*. Artech House, 475 pp.

Tomiyasu, K., 1978: Tutorial review of synthetic aperture radar with applications to the imaging of the ocean surface. *Proc. IEEE*, **66**, 563–583.

Way, J., and E. A. Smith, 1991: The evolution of synthetic aperture radar systems and their progression to the EOS SAR. *IEEE Trans. Geosci. Remote Sens.*, **29**, 962–985.

Zebker, H. A., and J. J. Van Zyl, 1991: Imaging radar polarimetry: A review. *Proc. IEEE*, **79**, 1583–1606.